

DUPLICATE

Numerical Weather Prediction



Forecasting Research Technical Report No. 358

A description of an AVHRR volcanic ash detection product and examples of its application

April 2001

S. Watkin

© Crown Copyright 2001

Met Office , NWP Division , Room 344 , London Road , Bracknell , Berkshire ,RG12 2SZ, United Kingdom

Forecasting Research
Technical Report No. 358

**A description of an AVHRR volcanic ash
detection product and examples of its
application**

by

S. Watkin

April 2001

The Met Office
NWP Division
Room 344
London Road
Bracknell
RG12 2SZ
United Kingdom

© Crown Copyright 2001

Permission to quote from this paper should be obtained from the
above Met Office division

Please notify us if you change your address or no longer wish to
receive these publications.

el: 44 (0)1344 856245 Fax: 44 (0)1344 854026 email: jsarmstrong@meto.gov.uk

A description of an AVHRR volcanic ash detection product and examples of its application

Sarah Watkin

Satellite Imagery Applications Group
NWP Division
Met Office

April 2001

Abstract

Volcanic ash clouds are a threat to aircraft safety. The London Volcanic Ash Advisory Centre, based at the Met Office, has a responsibility to issue advice to the aviation industry about the presence of volcanic ash in its designated area. To aid this task a volcanic ash detection product has been developed. This product displays the brightness temperature difference between two channels, at 10.8 and 12.0 μm , on the Advanced Very High Resolution Radiometer (AVHRR). Negative brightness temperature differences are expected for semi-transparent volcanic ash and positive brightness temperature differences for semi-transparent water and ice clouds. Images are produced for three areas including the London Volcanic Ash Advisory Centre area of responsibility. These are displayed on an internal web page and are updated throughout the day as data from AVHRR passes are received.

This report provides a description of the volcanic ash detection product and examples of situations that can affect the spectral signal in the imagery. Successful and failed detection of volcanic ash are discussed using examples from the eruptions of Mt. Spurr, Alaska in 1992, Soufriere Hills, Montserrat in 1997 and Hekla, Iceland in 2000. Several situations that cause false alarms have been identified and these are also discussed. A summary and ideas for future development of the volcanic ash product conclude this report.

Contents

1. Volcanic Ash Advisory Centre.....	3
2. Volcanic ash detection using AVHRR data.....	4
3. Data collected to study volcanic ash clouds.....	5
3.1 AVHRR data.....	5
3.2 TOMS data.....	8
4. Successful detection of volcanic ash.....	8
4.1 Eruption of Mt. Spurr, Alaska on 17 September 1992.....	9
4.2 Eruption of Soufriere Hills, Montserrat on 26 December 1997.....	11
5. Failure to detect volcanic ash in volcanic clouds.....	12
5.1 Eruption of Hekla, Iceland on 26 February 2000.....	13
6. False detection.....	17
7. The Autosat volcanic ash product.....	22
8. Summary and suggestions for further work.....	24
References.....	25
Glossary.....	27
Acknowledgements.....	27
Appendix.....	28

1. Volcanic Ash Advisory Centre

The London Volcanic Ash Advisory Centre (VAAC) is one of nine VAACs around the world. VAACs advise the aviation industry of the location and movement of volcanic ash clouds. They are designated by the World Meteorological Organisation and the International Civil Aviation Organisation. The London VAAC is operated by the Environment Monitoring And Response Centre (EMARC), in the National Meteorological Centre (NMC) of the Met Office. The VAAC is responsible for issuing volcanic ash advisories about the presence of volcanic ash within its area of responsibility (Figure 1). There are 18 volcanoes that have been active within the last 10,000 years in the London VAAC area of responsibility (Casadevall and Thompson, 1995).

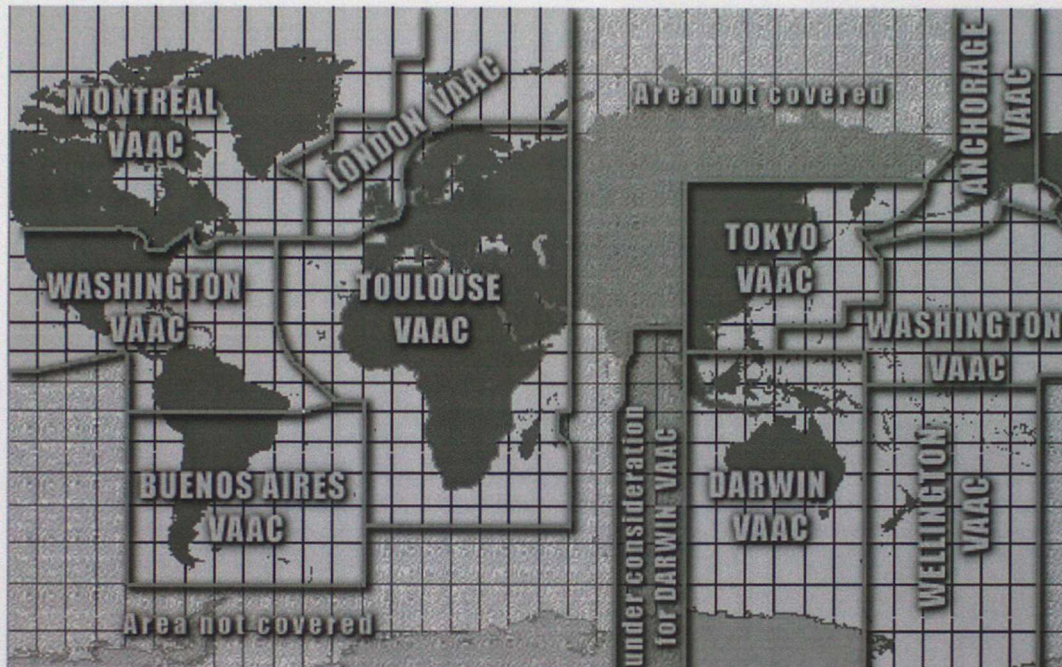


Figure 1. The Volcanic Ash Advisory Centres' areas of responsibility. From the Washington VAAC web site.

The major concern within the London VACC area is with eruptions from Icelandic volcanoes. These are generally well monitored from the ground and the London VAAC is notified when a volcano has erupted. The problem for the VAAC is to know whether volcanic ash was ejected, to what altitude and how it disperses. The best way of tracking volcanic ash clouds is with the use of satellite data.

The latest volcanic eruption to occur within the London VAAC area of responsibility was the eruption of Hekla in Iceland on 26 February 2000. This was a large eruption with the volcanic cloud rising to over 10 km (Rose et al., 2000). Volcanic ash advisories were issued by the London VAAC but they had difficulty in tracking the volcanic cloud using infrared and visible satellite imagery because a weather system moved over the area and the volcanic cloud was engulfed by meteorological cloud. This case is discussed later in the report.

The purpose of the work in the Satellite Applications group was to develop a volcanic ash detection product using AVHRR data to aid the staff in EMARC to track volcanic ash clouds, and to provide guidance on how to interpret the product.

2. Volcanic ash detection using AVHRR data

Volcanic clouds contain emissions from volcanic eruptions. They consist of varying amounts of water vapour and droplets, volcanic ash, sulphuric acid droplets, sulphur dioxide, and other gases (Oppenheimer, 1998). Volcanic ash can cause damage to aircraft, ranging from abrasion of surfaces to engine destruction. The composition of volcanic ash varies between eruptions, but the basic component is silicate based material (Prata, 1989). Thus, techniques for detecting the presence of volcanic ash are valuable in the prevention of aircraft damage and crashes. In addition to detecting the location of volcanic ash directly, the detection of sulphur dioxide (SO_2) may also assist in determining the region of danger for aircraft.

In this report the distinction is made between a volcanic cloud and a volcanic ash cloud. A volcanic cloud contains substances emitted by a volcano, it may or may not contain volcanic ash, whereas a volcanic ash cloud is a volcanic cloud that does contain volcanic ash.

Brightness temperature difference (BTD) data from channels in the 10-12 μm atmospheric window are frequently used to study volcanic ash clouds (e.g. Constantine et al., 2000, Schneider et al., 1999, Wen and Rose, 1994, Prata, 1989). Laboratory tests on volcanic ash samples found that the real and imaginary parts of the complex refractive index are smaller at 12.0 μm than at 10.8 μm (Deepak and Gerber, 1983). Assuming that these measurements are representative of ash in volcanic clouds it can be assumed that the emissivity of volcanic ash is smaller at 12.0 μm than at 10.8 μm . The converse has been found for water and ice particles, i.e. the real and imaginary parts of the complex refractive index are larger at 12.0 μm than at 10.8 μm (Warren, 1984). These characteristics can be used to discriminate between volcanic ash cloud and water or ice cloud. When the cloud is semi-transparent the radiation measured at the satellite contains a contribution from the surface and a contribution from the cloud. The differential absorption between 10.8 and 12.0 μm for volcanic ash, water and ice results in a brightness temperature (BT) difference between the two channels.

$\text{BTD} = \text{BT}_{10.8} - \text{BT}_{12.0} > 0$	for water and ice
$\text{BTD} = \text{BT}_{10.8} - \text{BT}_{12.0} < 0$	for volcanic ash

AVHRR (Advanced Very High Resolution Radiometer) is an imager carried on NOAA polar orbiting satellites that has a 1.1 km spatial resolution at nadir. AVHRR/2 is operational on NOAA 12 and 14 and has 5 channels: ch1 (0.63 μm), ch2 (0.87 μm), ch3 (3.7 μm), ch4 (10.8 μm) and ch5 (12.0 μm). AVHRR/3 is operational on NOAA 15 and NOAA 16 and has the same 5 channels with an additional channel (ch3a) centred at 1.6 μm . The 3.7 μm channel (ch3b on AVHRR/3) only operates at night, while ch3a operates during the day.

3. Data collected to study volcanic ash clouds

To study the signal due to volcanic ash in AVHRR channel 4 - channel 5 imagery, AVHRR data, and in some cases TOMS data, were collected for several volcanic eruptions. The TOMS data were used to help understand the behaviour of the signal in the AVHRR ch4-ch5 imagery.

3.1 AVHRR data

AVHRR data were retrieved from NOAA's Satellite Active Archive (SAA). This is an interactive archive on the Internet. The SAA stores AVHRR data from 1978 onwards mainly in Global Area Coverage (GAC) format. GAC pixels are sub-sampled, averaged values of the instrument field of view pixels (FOV), or Local Area Coverage (LAC) pixels (Figure 2). GAC has an effective spatial resolution at sub-satellite point of 4 km. Code was written to unpack, calibrate and geolocate the GAC AVHRR data using information from NOAA Polar Orbiter Data User's Guide (Kidwell, 1998) for AVHRR on satellites up to NOAA 14 and NOAA KLM User's Guide (Goodrum et al., 2000) for AVHRR on NOAA 15.

The use of GAC data rather than LAC data may introduce problems in the detection of volcanic ash clouds. For volcanic clouds that are homogeneous over an area of 16 km^2 or more, the sub-sampling and averaging will have little effect on the calculated brightness temperatures. This will be the case for most volcanic clouds that could be a threat to aircraft safety after the first few minutes of an eruption, although the cloud edges may be misrepresented.

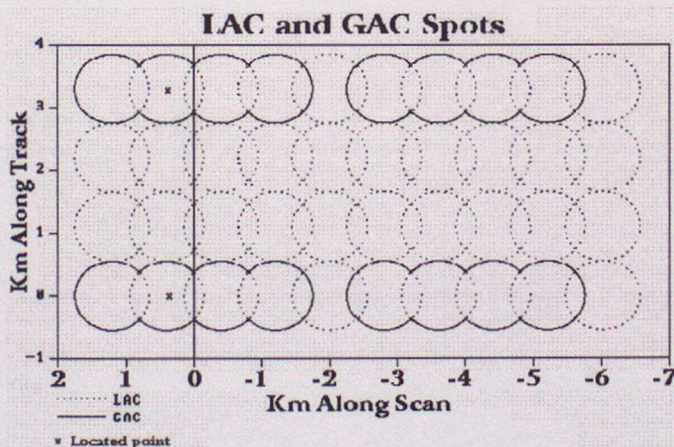


Figure 2. Earth locations of GAC and LAC pixels near nadir. GAC values are calculated on board the satellite by averaging four LAC values then skipping the fifth, then repeating, resulting in 409 GAC points along a scan. This is done for every third scan line. From NOAA KLM User's Guide.

The calibration code was tested using GAC and LAC data from NOAA 15 for the same scene. The LAC data were averages of several LAC pixels to coincide with the HIRS FOV for the purposes of a separate project. These data had been calibrated by the Satellite Meteorology Centre (CMS) in Météo-France. Only clear sky pixels over the ocean were compared since a homogeneous scene was required so that errors due to averaging would be small. It was found that the code written to calibrate the GAC data obtained from the SAA generated BT for channels 3, 4 and 5 that were within $\pm 0.04 \text{ K}$ of the BT from the LAC data. This proved that the errors in the calibration code were significantly smaller than observed brightness temperature differences for volcanic ash (typically -1 to -6 K).

Data were collected for 15 different volcanic eruptions. A range of eruptions were included, for example: Icelandic eruptions (since these are in the main area of interest for the London VAAC), large eruptions that have been well studied and documented, and eruptions in different climates. A summary of these cases is shown in Table 1. Channel 4 - channel 5 imagery was generated for all of these cases to determine the incidence of negative brightness temperature differences; these are also indicated in Table 1. Examples from these cases are shown later in this report.

Volcano	Eruption start date	Estimated maximum altitude of cloud (km)	Are significant negative ch4-ch5 BTDR present?	Is the volcanic cloud evident in ch4 imagery?	Length of time that the cloud could be tracked using ch4 and/or ch4-ch5 imagery
Bardarbunga, Iceland	02/10/96	4-5	No	Yes	1 day
Cerro Hudson, Chile	12/08/91	18	Yes	No	4.5 days
Etna, Italy	23/12/95	9.5	No	Yes	< 6 hours
Etna, Italy	01/06/00	3-4	No	Yes	3 hours
Fogo, Cape Verde Islands	03/04/95	2.5-5	No	No	0
Grimsvötn, Iceland	16/12/98	10	Yes	Yes	6 hours
Guagua Pichincha, Ecuador	05/10/99	18	Yes	Yes	< 7 hours
Guagua Pichincha, Ecuador	17/12/99	8	No	Yes	< 3 hours
Hekla, Iceland	17/01/91	11.5	No	No	0
Hekla, Iceland	26/02/00	11	No	Yes	2 hours
Jan Mayan, N. Atlantic	07/01/84	1	No	No	0
Pinatubo, Philippines	12/06/91	40	Yes	Yes	> 4.5 days
Soufriere Hills, Montserrat	26/12/97	15	Yes	Yes	1 day
Spurr, Alaska	17/09/92	>10	Yes	Yes	> 2.5 days
Stromboli, Italy	06/09/00	1	No	No	0

Table 1. AVHRR data were collected for the eruptions listed in the table. The eruption start date and estimated maximum altitude of the volcanic cloud were obtained from the Smithsonian Institution for all eruptions except for those of Cerro Hudson, Soufriere Hills and Spurr, where the information came from Constantine et al. (2000), Rose and Mayberry (2000) and the Alaska Volcano Observatory respectively. The last three columns refer to observations made from the AVHRR imagery obtained for each eruption. These are subjective observations made by the author and therefore may be interpreted differently by another observer. The final column containing an estimation of how long the volcanic cloud (rather than volcanic ash cloud) could be tracked is dependent on not only the signal in the imagery, but also the length of time between images (there is a long interval between passes in the tropics), and the length of time after the eruption for which images were collected, e.g. the Pinatubo eruption could possibly be tracked for longer than 4.5 days, but imagery was only collected for this length of time.

3.2 TOMS data

The Total Ozone Mapping Spectrometer (TOMS) has been carried on various polar orbiting satellites since 1979. Currently, the Earth Probe satellite carries the only operational instrument. The Earth Probe satellite orbits at an altitude of 740 km and covers the earth once per day (except for the winter pole). This compares to approximately 12 passes a day over Iceland from AVHRR on the NOAA polar orbiting satellites. The current TOMS instrument measures backscattered ultra-violet (UV) radiation in six wavebands centred at: 360.0, 331.2, 322.3, 317.5, 312.5, and 308.6 nm. The FOV is approximately $(39 \text{ km})^2$ at nadir. Earlier instruments had similar but slightly different channels. The technique for detecting volcanic ash and other UV absorbing aerosols uses a quantity called the Aerosol Index (AI) (Seftor et al., 1997):

$$AI = -100 \left[\log_{10} \left(\frac{I_{\lambda 1}}{I_{\lambda 2}} \right)_{meas} - \log_{10} \left(\frac{I_{\lambda 1}}{I_{\lambda 2}} \right)_{calc} \right]$$

Where I represents the upwelling radiation at the top of the atmosphere and $\lambda 1$ and $\lambda 2$ are the shortest and longest available wavelengths in the 330 to 400 nm range (where gaseous absorption is negligible). The AI is the difference in the measured and calculated values of the logarithms of the ratio of backscattered radiances at two UV wavelengths. The theoretical calculation is for a Rayleigh atmosphere over a Lambertian surface (Krotkov et al., 1999). For water clouds AI is approximately zero, for nonabsorbing aerosols AI is negative and for absorbing aerosols, such as volcanic ash, AI is positive and increases with optical depth and aerosol layer height. Situations where the TOMS AI may detect volcanic ash but the AVHRR ch4-ch5 technique may fail are: (i) when volcanic ash is overlying water/ice clouds or is in the presence of sub-pixel cloud, and (ii) when the volcanic ash cloud is opaque.

TOMS data can also be used to calculate a quantity called the sulphur dioxide index (SOI). The relative quantity of sulphur dioxide can be detected by its effects on ozone retrieval. The difference between the measured radiation and calculated radiation at particular UV wavelengths is determined. SO_2 absorption coefficients at 210 K are assumed and used with the difference calculations to determine whether SO_2 is present and in what quantity. The procedure involves some complex calculations that can be obtained from the Earth Probe TOMS Data Products User's Guide (McPeters et al., 1998).

4. Successful detection of volcanic ash

Volcanic ash clouds are successfully discriminated from water or ice clouds, and from clear skies, when negative ch4-ch5 BTD values occur caused by the wavelength dependent absorption properties of volcanic ash. The magnitude of the BTD values depends on several factors. The temperature difference between the surface and the cloud top is proportional to the BTD between channels 4 and 5. A low altitude ash cloud over a cold surface will produce a small magnitude ch4-ch5 BTD. The degree of transparency affects the magnitude of the ch4-ch5 BTD since this determines the contribution of the surface radiation to the measured radiances. An opaque or a extremely sparse volcanic ash cloud will give BTD close to zero. The amount of water vapour in the atmosphere both below and above the ash cloud will also affect the magnitude of the observed BTD. Water vapour has reverse differential absorption characteristics to ash in the 10.8 and 12.0 μm channels and therefore acts to move the BTD signal in the positive direction. High altitude ash clouds in dry atmospheres are likely to give a larger magnitude BTD than a low altitude cloud in a

moist atmosphere. Similarly the proportion of water vapour, liquid water and ice within the volcanic cloud affects the BTB signal. These factors are discussed in more detail in section 5 on failure to detect volcanic ash clouds.

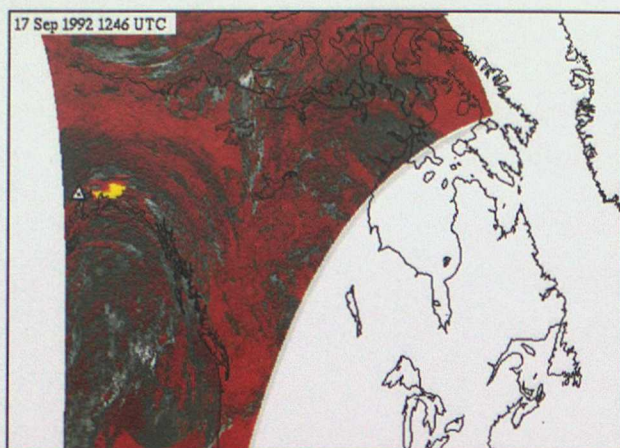
From the 15 eruptions that were studied (Table 1) only 6 gave significant negative ch4-ch5 BTBs. Two of these eruptions are discussed below. Significant negative BTBs are those that are different to the background ch4-ch5 BTB values by at least -1 K. A correlation can be seen between the altitude of the volcanic cloud and the occurrence of significant negative BTBs. In general, ash in volcanic clouds that reach above 10 km in altitude is more likely to be detected in ch4-ch5 BTB imagery than ash in volcanic clouds below 10 km altitude.

4.1 Eruption of Mt. Spurr, Alaska on 17 September 1992

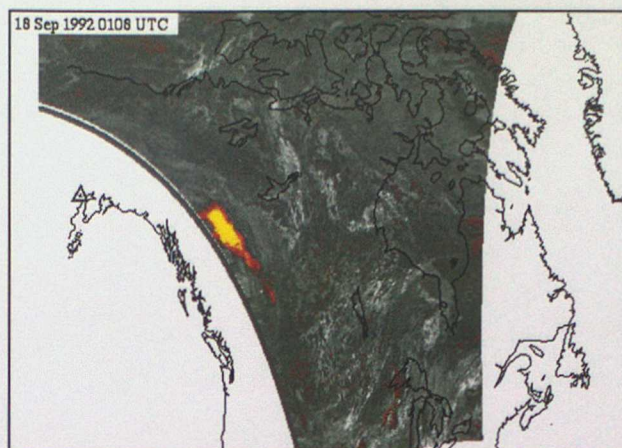
The eruption of Mt. Spurr in Alaska, U.S.A. (61.30° N, 152.25° W) in September 1992 is a good example of the successful detection of a volcanic ash cloud. Using AVHRR ch4-ch5 imagery the ash cloud resulting from the eruption of Mt. Spurr can be tracked for 2.5 days as it travels across North America (Figure 3).

Late in the day on 16 September 1992 (approximately 12 noon UTC, 17 September 1992) an eruption occurred that lasted 3.5 hours (Alaska Volcano Observatory). The first image, shortly after the eruption, at 1246 UTC, (Figure 3(a)) shows strongly negative BTBs to the east of the volcano. The ash cloud is carried approximately 3000 km to the south-east over the Canada/U.S.A. border (Figure 3(c)), and then changes direction and is transported in a north-easterly direction. At 1252 UTC on 19 September 1992 (Figure 3(e)) the ash cloud stretches from Lake Michigan towards Hudson Strait, a distance of approximately 2400 km. At this time (Figure 3(e)), when the ash cloud was approximately 48 hours old, a minimum BTB of -19.2 K was observed. The final image from the data collected is at 0704 UTC on 20 September 1992, 66 hours after the first image showing the volcanic ash cloud (Figure 3(f)). Negative ch4-ch5 BTB values are still prominent indicating that there is still a significant volume of ash present. The ash cloud could possibly be tracked for a longer period of time, but data were not collected beyond the time of the final image shown.

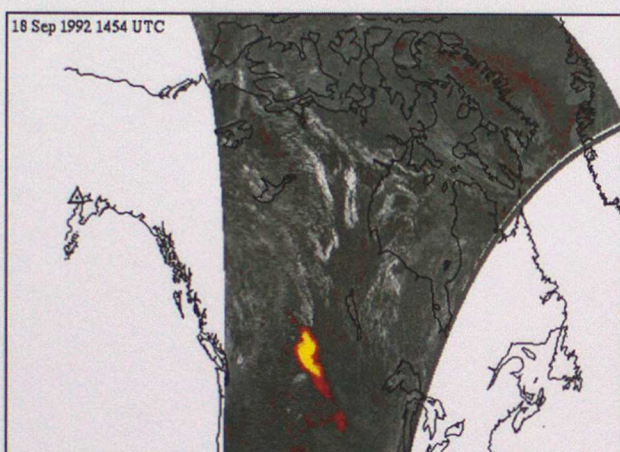
Some of the images in Figure 3, notably (a) and (f) have a higher occurrence of negative BTB values scattered across the image than the other images. Images (a), (e) and (f) are from the AVHRR instrument on NOAA 11, the others are from AVHRR on NOAA 12. The higher occurrence of negative values in the images from NOAA 11 are believed to be due to errors associated with the instrument (see section 6 on false detection).



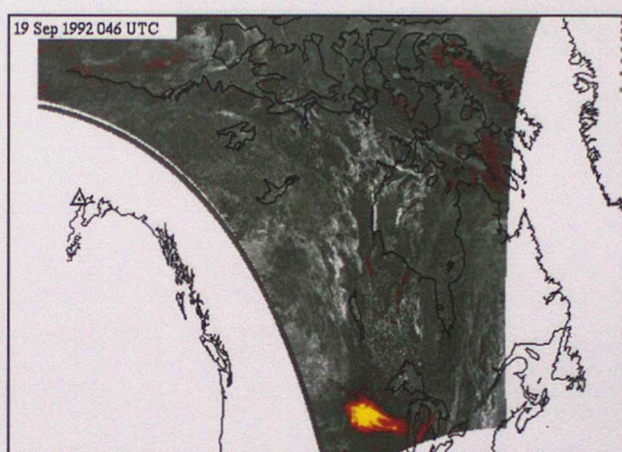
(a) 17 September 1992 1246 UTC (NOAA 11)



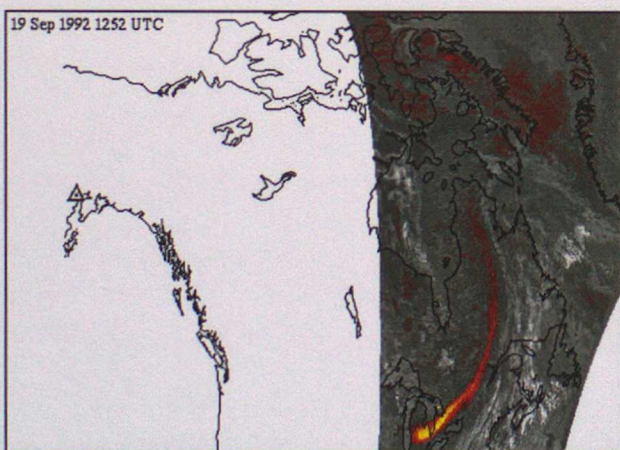
(b) 18 September 1992 0108 UTC (NOAA 12)



(c) 18 September 1992 1454 UTC (NOAA 12)



(d) 19 September 1992 0046 UTC (NOAA 12)



(e) 19 September 1992 1252 UTC (NOAA 11)



(f) 20 September 1992 0704 UTC (NOAA 11)

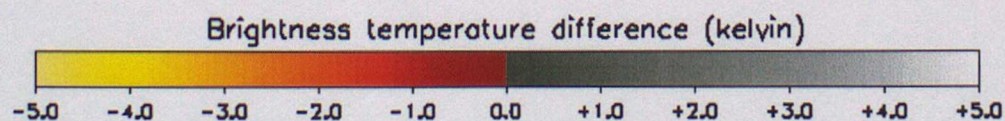


Figure 3. AVHRR ch4 - ch5 imagery of the volcanic ash cloud from the eruption of Mt. Spurr, Alaska, U.S.A. (marked by a triangle). Minimum BTD values for the volcanic ash cloud are -14.2, -14.0, -8.3, -10.3, -19.2 and -4.5 K for images (a) to (f) respectively.

4.2 Eruption of Soufriere Hills, Montserrat on 26 December 1997

The magnitude of the negative ch4-ch5 BTD varies between eruptions and as a volcanic cloud evolves. Figure 4 shows an example of an ash cloud that gave a weakly negative ch4-ch5 signal. The eruption of Soufriere Hills on Montserrat (16.72°N, 62.18°W) in December 1997 ejected volcanic ash and sulphur dioxide. The volcanic ash signal in the AVHRR ch4-ch5 imagery is weak in comparison with the strength of the signal due to the Mt. Spurr ash cloud. The minimum BTD in Figure 4 is -1.9 K, a factor of 10 smaller in magnitude than the minimum BTD observed for the Mt. Spurr ash cloud. Rose and Mayberry (2000) estimated the total ash mass to be approx. 5×10^9 kg (0.01 % of this as fine ash in the size range 1-25 μm) for the Soufriere Hills eruption on 26 December 1992 compared to approx. 30×10^9 kg (0.02% of this as fine ash) for the Mt. Spurr eruption on 17 September 1992. The larger ash particles comprise most of the mass ejected from the volcano, but these quickly fall to earth leaving the fine ash particles which can remain in the atmosphere for a long time. The AVHRR ch4-ch5 technique is only sensitive to ash particles smaller than 5-10 μm (Wen and Rose, 1994; Prata, 1989). The smaller mass of fine particles contributes to the smaller negative BTD in the Soufriere Hills eruption. Another consideration in the sensitivity of this technique is the atmospheric conditions. Montserrat is situated in the eastern Caribbean Sea and has a tropical climate with high humidity. Volcanic cloud pixels with low optical depth in the moist tropical atmosphere could have their BTD shifted by as much as + 3K (Rose and Prata, 1997).

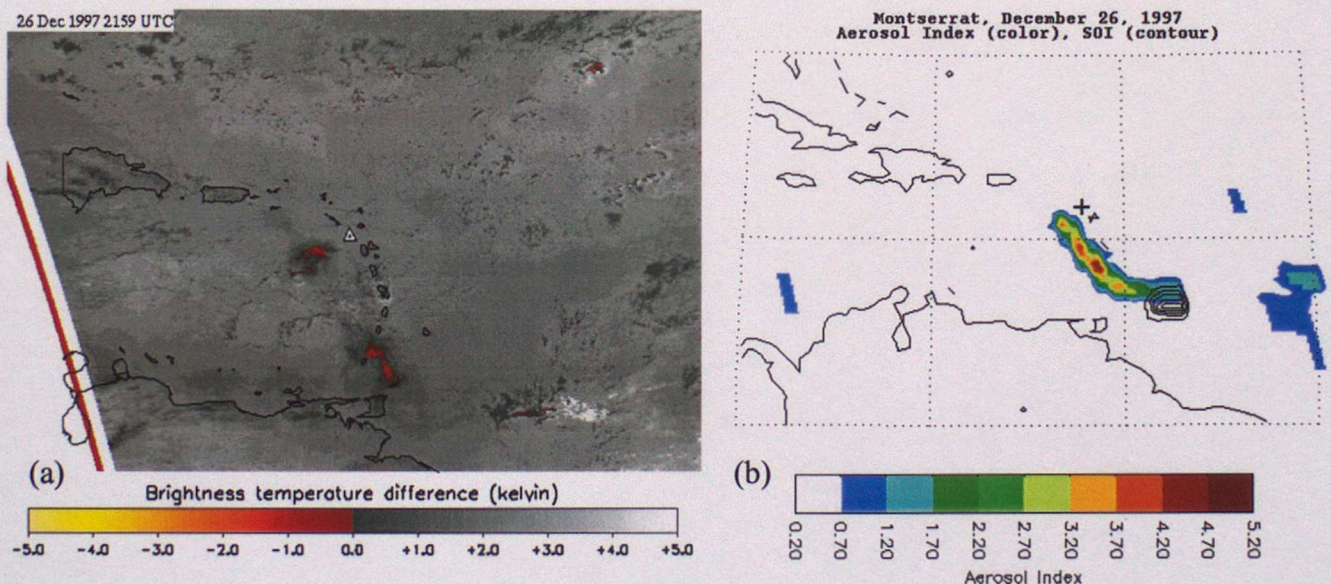


Figure 4. Images of the volcanic cloud from Soufriere Hills, Montserrat on 26 December 1997. Figure 4(a) is an AVHRR ch4-ch5 BTD image at 2159 UTC indicating the location of volcanic ash by slightly negative pixels (red). Figure 4(b) is an image derived from TOMS data recorded at 1543 UTC. The coloured areas show where the aerosol index is greater than 0.7, and the black contours show the location of the sulphur dioxide. Source of Figure 4(b): TOMS SO₂ and Ash Group at NASA Goddard Space Flight Center (<http://skye.gsfc.nasa.gov/index.html>).

The image in Figure 4(b) is generated from TOMS data. The coloured areas show the position of the aerosols (volcanic ash) at this time. Taking into account the slightly different map areas and projections and the difference in time (about 6 hours) the positions of the volcanic ash signal in the AVHRR ch4-ch5 image (Figure 4(a)) and the signal in the TOMS image are reasonably well correlated. The major difference is that the volcanic ash signal in the AVHRR ch4-ch5 image does not cover as large an area as the signal in the TOMS image. The smaller coverage in Figure 4(a) is

likely to be caused by the volcanic ash signal being masked by the high water vapour content of the lower troposphere. Water vapour in the atmosphere does not strongly affect the signal in the TOMS data. This illustrates the major weakness of the AVHRR ch4-ch5 detection technique, and the comparative strength of the TOMS data.

It can also be seen from Figure 4(b) that the sulphur dioxide emissions are not coincident with the volcanic ash emissions. The region of high sulphur dioxide concentration lies slightly south-east of the main area of volcanic ash. This separation could be due to: (a) different emission times, (b) gravitational separation of ash within the volcanic cloud or (c) interaction of ash particles with liquid water causing accelerated sedimentation (Rose and Mayberry, 2000). Both (b) and (c) result in horizontal separation if vertical wind shear is present. The separation of the sulphur dioxide from the volcanic ash portion of volcanic clouds has been observed in several cases, e.g. Cerro Hudson eruption in August 1991 (Constantine et al., 2000), El Chichón eruption in April 1982 (Schneider et al., 1999). The position of the sulphur dioxide cloud resulting from an eruption can not always be relied upon to indicate the position of the volcanic ash cloud. Furthermore, sulphur dioxide may be ejected without volcanic ash or vice versa.

5. Failure to detect volcanic ash in volcanic clouds

Volcanic clouds cannot be discriminated from water or ice clouds using AVHRR ch4-ch5 imagery if they do not produce a negative BTM signal. In addition to the problem of knowing the location of the volcanic cloud, it is not possible to tell if there is ash present in the volcanic cloud.

Circumstances that reduce the magnitude of the volcanic ash signal (see section 4) can also cause the BTM signal to become positive, these and other factors are listed below.

- (1) When there is no ash present in the volcanic cloud, then soon after the eruption it will resemble a water or ice cloud with positive BTM values. After some time, hours to days, sulphuric acid aerosol can form in volcanic clouds from the oxidation of sulphur dioxide. This usually occurs if a volcanic cloud reaches the stratosphere. Sulphuric acid aerosols have similar absorption characteristics to volcanic ash and therefore can give negative BTM.
- (2) Water or ice clouds and high humidity in the atmosphere can cause positive BTM values to occur. Water in the troposphere absorbs infrared radiation emanating from the earth's surface and the volcanic ash cloud. All phases of water absorb a greater proportion of radiation at 12.0 μm than at 10.8 μm and thus can reverse the signal from the volcanic ash cloud.
- (3) Volcanic clouds are composed of water vapour and droplets, silicate ash, sulphuric acid droplets, sulphur dioxide, and other gases (Oppenheimer, 1998). The proportion of these different components affects the spectral response of the overall volcanic cloud. If there is a large proportion of water vapour in the volcanic cloud then the ch4-ch5 BTM signal due to the ash component may be reduced or masked completely. The fine ash particles can act as cloud condensation nuclei so that the cloud resembles a water or ice cloud, depending on the cloud temperature. Rose et al. (1995) studied the eruption of Rabaul in 1994, which produced a volcanic cloud with positive ch4-ch5 BTM. Using comparisons with radiative transfer calculations they found that Rabaul's cloud had the spectral characteristics of spherical ice particles. They conclude that the ice signal in the AVHRR imagery is explained by ash being encased within ice in the volcanic cloud. The water vapour may emanate from the interior of the volcano, surface water, or entrainment of moist air as the cloud rises. It is thought that most of the water vapour in a volcanic cloud comes from the entrainment of moist air (Bill Rose, personal communication).

5.1 The eruption of Hekla, Iceland on 26 February 2000

An example of a volcanic cloud that could not be identified as containing ash using AVHRR ch4-ch5 imagery was from the eruption of Hekla in Iceland (63.98°N, 19.70°W) in February 2000. The information in the following description of the eruption was obtained from the Smithsonian Institute. On 26 February a 6-7 km long fissure on Hekla opened up and started erupting at 1819 UTC. It was reported that this produced an ash cloud that rose to 11 km altitude in only 6 minutes and it was carried to the north. Ashfall was recorded on an island 300 km north of Hekla. The eruption continued sporadically until 29 February 2000.

AVHRR ch4-ch5 imagery of the volcanic cloud from the Hekla eruption is shown in Figures 5 and 6. Data were collected from 1806 UTC on 26 February until 0714 UTC on 29 February 2000. The images in Figure 5 were recorded soon after the start of the eruption. The timestamp of 1806 UTC refers to the time that the first line of the image for this orbit was recorded. The infrared (channel 4) image (Figure 5(a)) and ch4-ch5 image (Figure 5(b)) show the volcanic cloud to be optically thick in the infrared with a low brightness temperature of 203 K or less, indicating its high altitude. The edges of the volcanic cloud are semi-transparent since they produce positive ch4-ch5 BTD with a large magnitude (≥ 5 K). At this time the volcanic cloud can be clearly seen in these images even though there are no negative ch4-ch5 BTD pixels indicative of volcanic ash.

12 hours later a low pressure system had moved north across Iceland and had engulfed the volcanic cloud. The frontal cloud associated with the low pressure system is clearly visible in the infrared image at 0552 UTC on 27 February (Figure 6(a)), but the previous days volcanic cloud cannot be distinguished from the frontal cloud. There is a small area near the volcano with low brightness temperatures possibly indicating that Hekla was still erupting. The AVHRR ch4-ch5 image (Figure 6(b)) does not assist with the detection of the volcanic cloud. An area of large positive BTD (≥ 5 K) is present to the north of Iceland aligned in an east-west direction. These positive values are consistent with the presence of ice particles in a semi-transparent cloud. None of the AVHRR ch4-ch5 images exhibited signs of volcanic ash.

The TOMS SO₂ and Ash Group, based at the NASA Goddard Space Flight Center created imagery for the Hekla eruption showing the quantity of SO₂ in the atmosphere (Figure 7). These indicate that there was a significant amount of sulphur dioxide ejected during the eruption. If it is assumed that the position of the sulphur dioxide represents the position of the volcanic cloud (this assumption is questionable, as discussed in section 4.2) then on 27 February the volcanic cloud is in the vicinity of the large region of semi-transparent ice cloud indicated in the ch4-ch5 image (Figure 6(b)). A day later, on 28 February the position of the sulphur dioxide plume in Figure 7(b) is over the Barents Sea.

Based on the imagery presented, there is no evidence that there was ash in the volcanic cloud. However, the volcanic cloud did contain a large quantity of sulphur dioxide and water vapour. Ash was reported to have fallen 300 km north of Hekla (Smithsonian Institute). This may indicate that there were some coarse ash particles in the eruption cloud, but that sedimentation meant that they did not remain in the volcanic cloud for long. The ch4-ch5 detection technique would not have detected coarse ash particles ($> 10 \mu\text{m}$). The water vapour could have been ejected during the eruption, or it may have been entrained from the moist air associated with the low pressure system. Rose et al. (2000) studied AVHRR, MODIS and TOMS data of the Hekla eruption, and also material collected from the filters from the engine of a NASA DC8 aircraft that unexpectedly flew through the volcanic cloud. They also reach the conclusion that there was little or no fine ash in the volcanic cloud and that moist tropospheric air was entrained into the volcanic cloud. They suggest

that the abundance of sulphate aerosol acted as cloud condensation nuclei in the unusually moist stratosphere, forming ice cloud. In addition to the evidence from the satellite imagery the results from scanning electron microscope studies of material collected from the aircraft filters and cloud condensation nuclei measurements taken from a different aircraft both conclude that there is no firm evidence for the presence of silicate ash in the volcanic cloud.

The London VAAC issued Volcanic Ash Advisories for this eruption. Since conventional satellite imagery (i.e. single channel infrared and visible imagery) was of little use in tracking the volcanic cloud these were based on the output from the Met Office Nuclear Accident Model (NAME). NAME is used to simulate the medium and long range transport of airborne pollutants. The model provides estimates of air concentrations and of the deposition of pollutants to the ground. The output from NAME for 12, 24, 36, 48, 60 and 72 hours after the start of the eruption of Hekla is shown in Figure 8. These predictions generally compare well with the locations of the sulphur dioxide plume from the TOMS data.



Figure 5. AVHRR imagery on 26 February 2000 at 1806 UTC. Figure (a) is an infrared (ch4) image with white indicating low BT and black indicating high BT. Figure (b) is a ch4-ch5 image with grey indicating positive BTD ($\text{white} \geq +5 \text{ K}$), and red to yellow indicating negative BTD values ($\text{yellow} < -5 \text{ K}$). The position of Hekla on Iceland is shown by the white triangle.

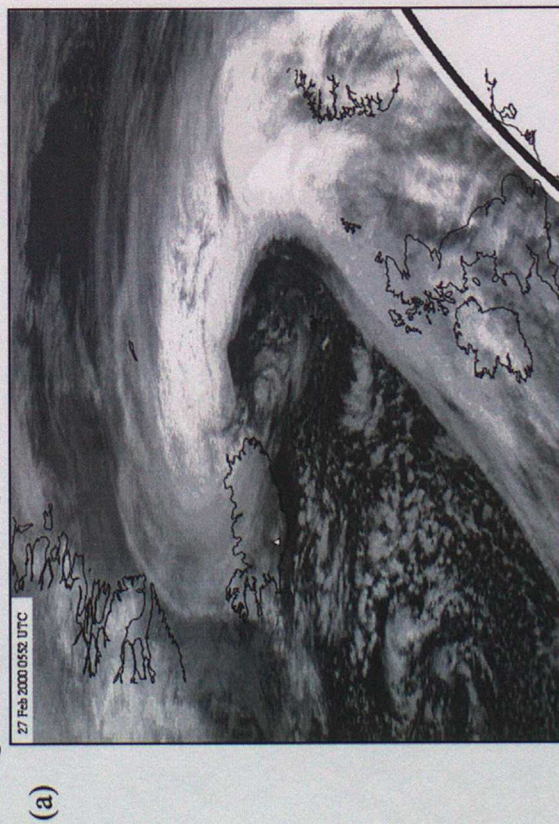


Figure 6. AVHRR imagery on 27 February 2000 at 0552 UTC. Annotation is the same as for Figure 5.

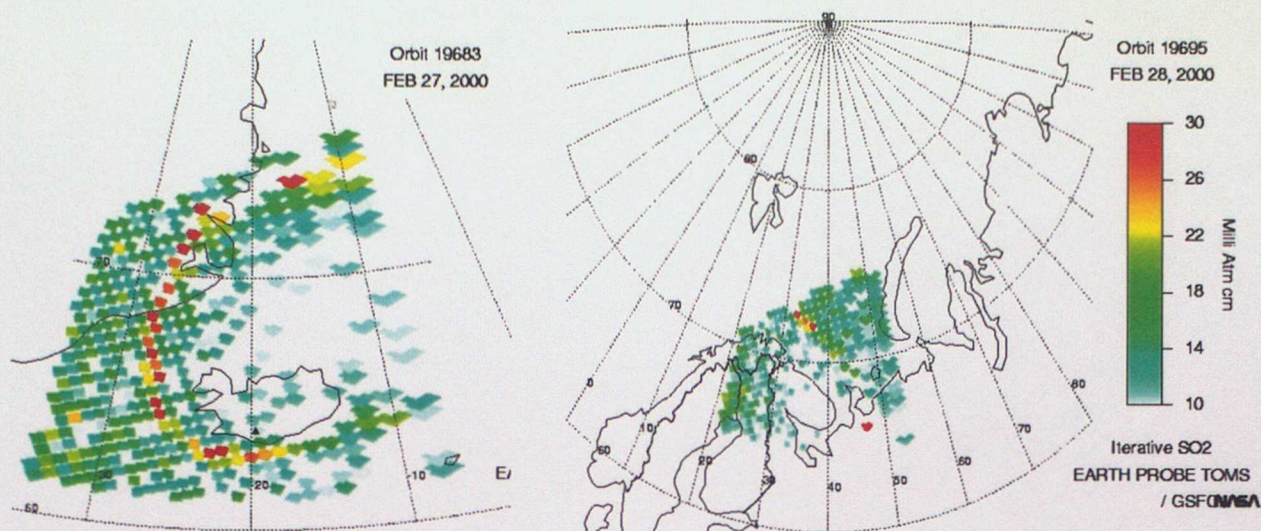


Figure 7. SO_2 plots generated from TOMS data of the volcanic cloud from the eruption of Hekla, Iceland. The image on the left was taken on 27 February 2000 at 1157 UTC, and the image on the right on 28 February 2000. From the TOMS SO_2 and Ash Group at the NASA Goddard Space Flight Center.

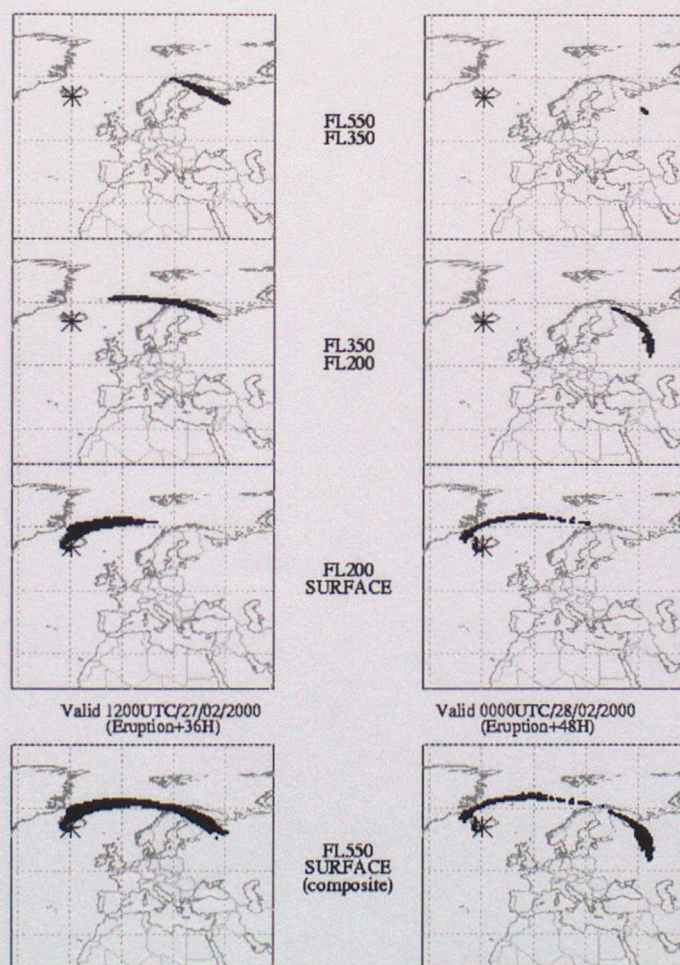


Figure 8. A re-run of the NAME model shows the predicted location of the ash from Hekla at different flight levels (FL) for 36 and 48 hours after the start of the eruption.

6. False detection

To use AVHRR ch4-ch5 imagery to detect volcanic ash clouds it is important to understand that there are other situations that can cause negative BTD values in the imagery. The ch4-ch5 imagery is of little use in detecting and tracking volcanic ash clouds if the false alarm rate is high, that is when there is a high occurrence of negative ch4-ch5 BTD that have the appearance of volcanic ash clouds. By studying AVHRR ch4-ch5 imagery, three situations that cause negative ch4-ch5 BTD have been determined: mineral dust clouds, situations in which the surface emissivity is greater at 12.0 μm than at 10.8 μm and channel misalignment. There are likely to be other situations that may be identified after further investigations.

A situation that can cause negative ch4-ch5 BTD is when atmospheric constituents have similar absorption properties to those of volcanic ash clouds. AVHRR ch4 and ch5 images have been used to study mineral dust aerosols in the atmosphere. Ackerman (1997) reports that negative BTD values are observed to occur for dust storms over the Arabian Peninsula, Africa and the south-west United States. A cloud composed of mineral dust aerosols resulting from a surface dust storm could resemble a volcanic ash cloud (Figure 9). But this is unlikely to affect the tracking of volcanic ash clouds resulting from eruptions in the North Atlantic and is more of a problem for tropical and sub-tropical regions.



Figure 9. AVHRR ch4-ch5 BTD image over the western part of the Mediterranean Sea on 25 August 2000. Grey to white are positive BTD values, red are negative BTD values. A mineral dust cloud can be seen over the Algerian coast with values of approximately -2 K.

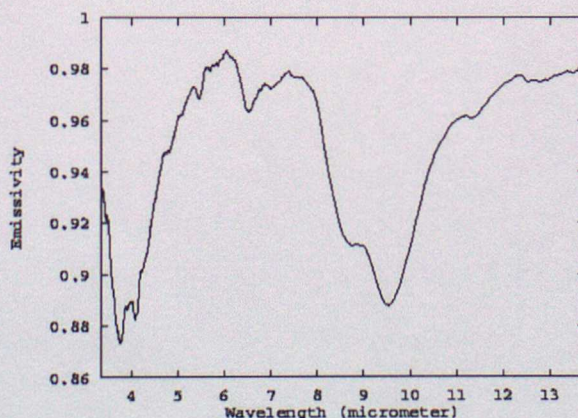


Figure 10. Emissivity as a function of wavelength measured in a laboratory from some soil samples collected in Death Valley, U.S.A.. From MODIS (Moderate Resolution Imaging Spectrometer) UCSB Emissivity Library (<http://www.icesb.ucsb.edu/~zhang/EMIS/html/em.html>).

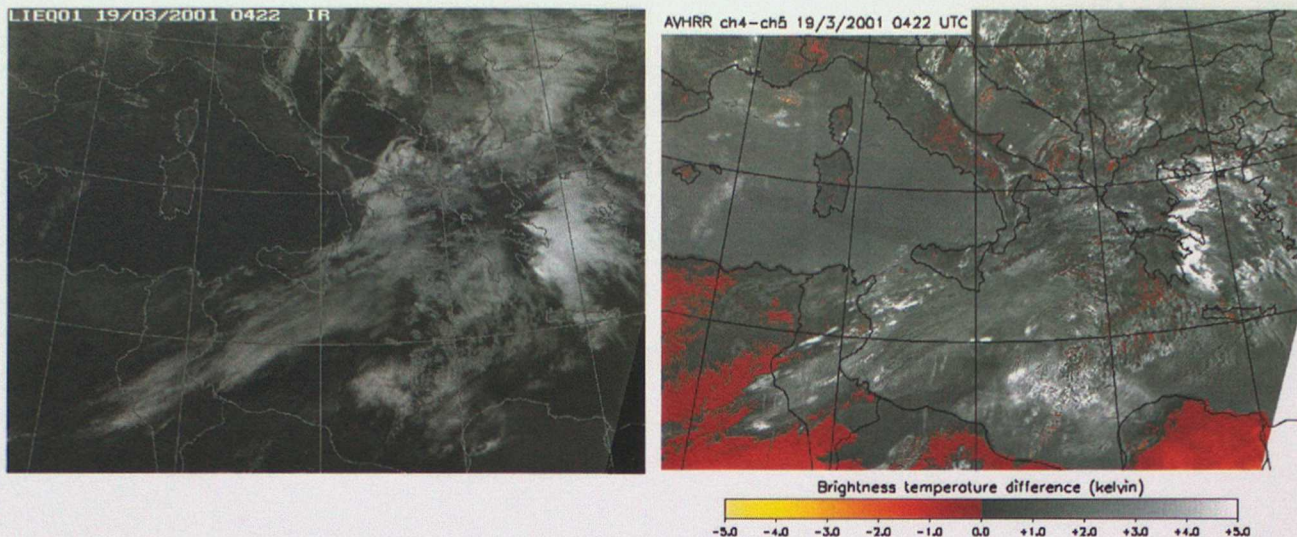


Figure 11. AVHRR ch4 (left) and ch4-ch5 (right) over the Mediterranean area on 19 March 2001 at 0422 UTC. The ch4 image displays low brightness temperatures as white, and high brightness temperatures as black. Large areas of negative pixels (red to yellow) can be seen in the ch4-ch5 image over the clear areas of land. The land at the bottom of the image is in the northern areas of the Saharan desert.

In clear sky situations and with negligible atmospheric absorption the radiance measured at the satellite depends only on the surface characteristics. The surface emissivity is a function of wavelength, surface type and viewing angle. If the surface emissivity is greater at $12.0\ \mu\text{m}$ ($\epsilon_{12.0}$) than at $10.8\ \mu\text{m}$ ($\epsilon_{10.8}$) then the brightness temperature measured at the satellite will also be greater at $12.0\ \mu\text{m}$ than at $10.8\ \mu\text{m}$, thus giving a negative ch4-ch5 BTD. Surface emissivities are difficult to determine, but some laboratory measurements have been made. It is known that in many arid desert regions $\epsilon_{12.0} > \epsilon_{10.8}$ (Prata, 1989; Ackerman, 1997). An example of emissivity measurements made in a laboratory for a soil sample collected from Death Valley in U.S.A. is shown in Figure 10. The plot of emissivity against wavelength shows increasing emissivity between 10.8 and $12.0\ \mu\text{m}$. Large areas of negative BTD values have been observed to frequently occur over clear regions of North Africa (Figure 11). The soil in the Northern area of the Saharan desert is likely to have similar emissivity characteristics to that in Death Valley. Another region where negative BTD values frequently occur is over some glacial regions of Greenland (examples can be seen in Figure 12). This may also be a result of the differences in the surface emissivities at the two wavelengths. Although these regions of negative BTD may resemble volcanic ash clouds in some circumstances they are unlikely to be confused with volcanic ash clouds near the start of the eruption since the volcanic ash cloud is likely to be visible in the infrared image. As the cloud disperses the optical depth at infrared wavelengths will decrease, but if the cloud travels over a region with these surface characteristics then the signal due to the volcanic ash may still stand out against the background BTD values.

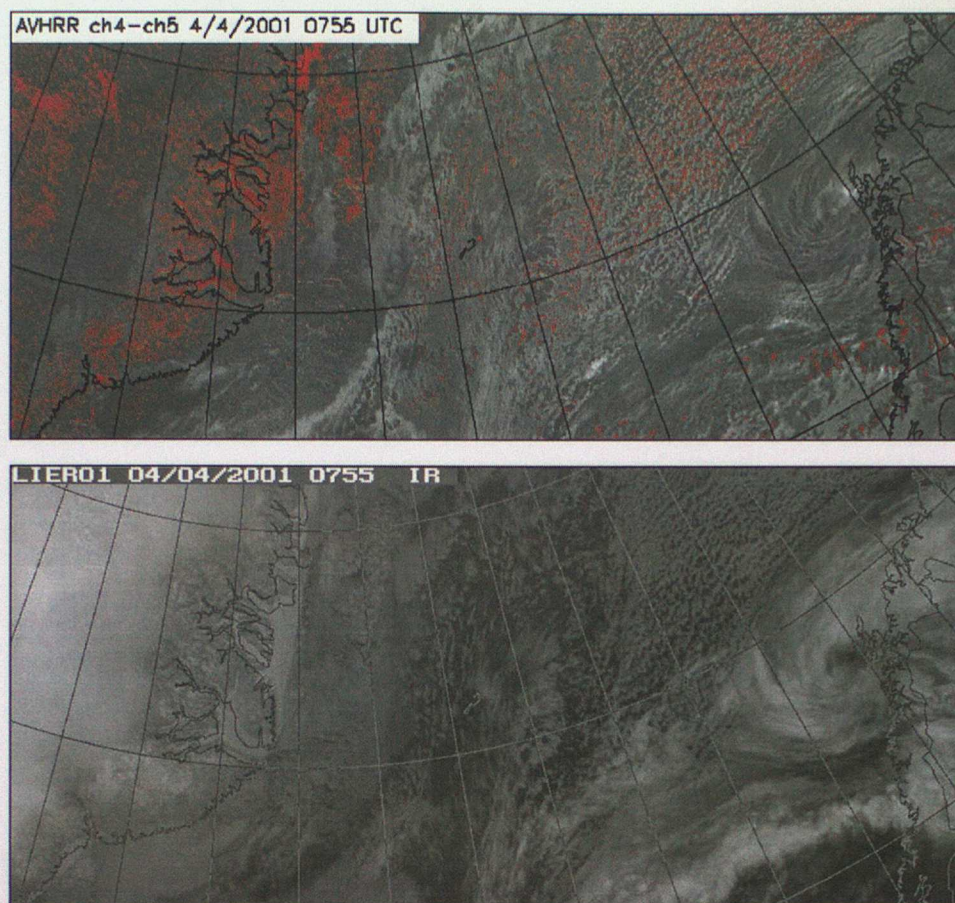


Figure 12. AVHRR ch4-ch5 (top) and channel 4 (bottom) images over the North Atlantic Ocean on 4 April 2001. The ch4-ch5 image shows a scattering of negative pixels (red) associated with the small scale broken cloud that can be seen in the infrared (channel 4) image. There are also many negative pixels over land and along the coast of Greenland (on the left of each image).

A frequent observation in AVHRR ch4-ch5 imagery is that negative BTD occur along the edges of some small scale clouds (Figure 12). This appears to be due to the misalignment of AVHRR channels 4 and 5. Only in regions where there is sub-pixel cloud or cloud edges does the misalignment between the two channels cause a BTD. When two channels are misaligned with respect to one another then each channel is sensing radiation from a slightly different scene. In homogeneous areas, e.g. clear sea and complete cloud cover, the misalignment does not affect the value of the BTD. Only in inhomogeneous areas where individual fields of view (FOV) can contain regions with different brightness temperatures can BTD be caused by the misalignment between the channels.

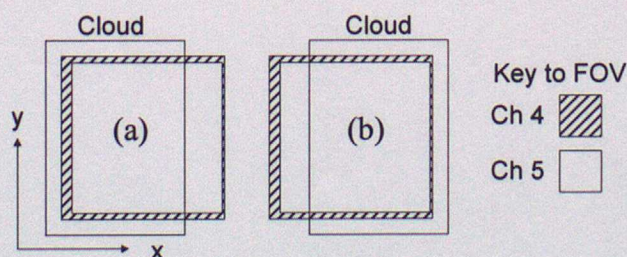


Figure 13. Schematic of the alignment of the channel 4 and channel 5 FOV for AVHRR on NOAA 14. Square FOV are assumed with channel 5 FOV displaced in the positive x direction relative to channel 4. Two situations are considered: (a) cloud covering the left side of the FOV, and (b) cloud covering the right side of the FOV. In this schematic the size of the channel 5 FOV is smaller than the channel 4 FOV, as is the case for AVHRR on NOAA 12 and 14 (see Table 2).

		Field of view (one dimension of a square)				Misalignment ch4 and ch5		FOV area ch4 - FOV area ch5	Cloud fraction in ch 5 FOV, if there is 0.5 cloud fraction in ch 4 FOV	
NOAA Sat ID & AVHRR instrument		Ch4 (mrad)	Ch4 (m)	Ch5 (mrad)	Ch5 (m)	mrad	m	m ²	Figure13 (a)	Figure 13 (b)
12	2	1.41	1175	1.30	1083	0.016	14	208 x 10 ³	0.487	0.513
14	2	1.41	1175	1.30	1083	0.037	31	208 x 10 ³	0.471	0.529
15	3	1.3	1083	1.3	1083	0.059	49	0	0.455	0.545
16	3	1.3	1083	1.3	1083	0.031	26	0	0.476	0.524

Table 2. Field of view measurements for channels 4 and 5 on AVHRR instruments on different NOAA satellites. Calculations assume square FOV, nadir viewing and a satellite altitude of 833 km. The last two columns refer to the two situations drawn in Figure 13.

Schematics of the centres of the FOV for all the AVHRR channels for different satellites were obtained from the National Climatic Data Center at NOAA. These illustrate the relative alignment of the channels. The design specification is for all of the AVHRR channels to be aligned to within 0.1 milliradian (mrad) of each other. All the AVHRR instruments that were studied came within this specification. The FOV schematics for the AVHRR instruments on NOAA 12, 14, 15 and 16 are presented in the Appendix. The misalignments between channel 4 and channel 5 for the four instruments were determined from these plots. The actual dimensions of the FOV were obtained from the NOAA Polar Orbiter Users' Guide (Kidwell, 1998) for NOAA 12 and 14, and from NOAA KLM Users' Guide (Goodrum, 2000) for NOAA 15 and 16. The infrared detectors on AVHRR are square but the angular response functions for these detectors indicate that the FOVs have rounded corners (Kidder and Vonder Haar, 1995). For convenience square FOVs have been considered in the calculations described here. The general arguments and conclusions drawn from the calculations are valid for rounded FOV shapes, but the magnitude of some of the calculations will vary. The difference in the areas of the square FOV between the two channels were calculated. The cloud fraction in the channel 5 FOV was calculated for a cloud fraction in the channel 4 FOV of 0.5. Two figures were calculated, one for each of the situations in Figure 13. Figures for the four AVHRR instruments are presented in Table 2.

Brightness temperature difference calculations were performed for different cloud fractions, varying from 0.0 to 1.0 in channel 4 FOV. The satellite observed radiance contains contributions from the surface and from the cloud. The Planck function was used to calculate the blackbody radiation $B(T)$ at 10.8 and 12.0 μm for a surface temperature of 285 K and a cloud top temperature of 235 K. The surface and cloud emissivities were assumed to be 1.0 and the atmospheric contribution to the radiance assumed to be negligible. Radiances (I_λ) were calculated for the central wavelength (λ) of each channel assuming different cloud fractions (A_λ) for both situations in Figure 13, using:

$$I_\lambda = (1 - A_\lambda)B(T_s) + A_\lambda B(T_c)$$

The radiance is converted to brightness temperature by inverting the Planck function, and then the BT difference between channels 4 and 5 is calculated. Plots of the BT difference against channel 4 cloud fraction are shown in Figure 14 for AVHRR instruments on NOAA 12, 14, 15 and 16.

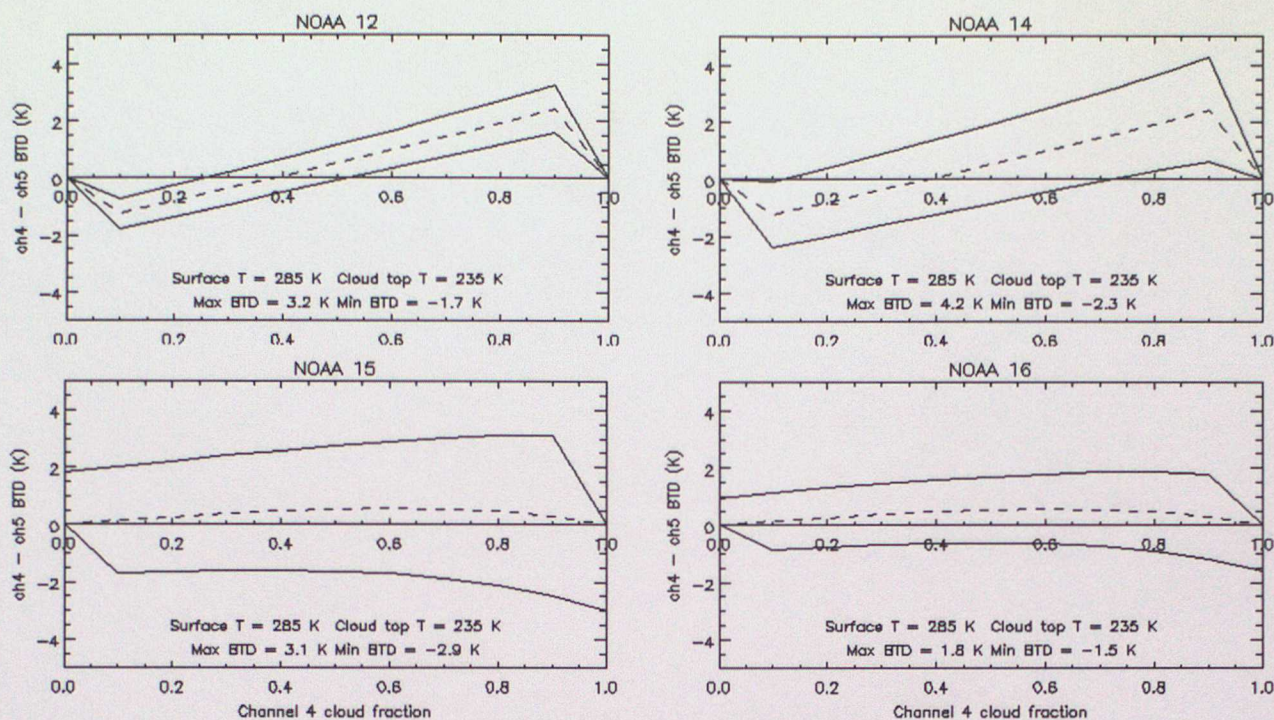


Figure 14. Graphs of ch4-ch5 BTD against channel 4 FOV cloud fraction. The values were calculated for the AVHRR instruments on NOAAs 12, 14, 15 and 16. Actual values for each of these instruments of FOV areas (assuming square FOV) and misalignment were used. The two solid lines plotted in each graph refer to the two arrangements of the channel FOV as shown in Figure 13. In all graphs the top line is for situation (b) and the lower line for situation (a) in Figure 13. The dotted line in each graph shows the BTD values if there were no misalignment between channels 4 and 5.

The graphs in Figure 14 demonstrate that the misalignment of channels 4 and 5 on AVHRR can cause positive and negative BTD values with a larger magnitude than the BTD expected when there is no misalignment between the channels. The graphs for NOAA 15 and 16 have a different form from the graphs for NOAA 12 and 14. For AVHRR on NOAA 12 and 14 the area of the FOV is smaller for channel 5 than for channel 4, so that when the cloud fraction in channel 4 is 0.0 or 1.0, the cloud fraction in channel 5 is also 0.0 or 1.0. However, for AVHRR on NOAA 15 and 16 the areas of the FOV are identical for channel 4 and channel 5, thus a BTD can occur even when the cloud fraction in channel 4 is 0.0 or 1.0. For the input values used in the calculations the minimum BTD is between -1.5 K and -2.9 K for the four instruments. These values are comparable with values observed for volcanic ash. The misalignment of the two channels causes negative BTD values in the imagery with a distinct spatial pattern. Visual inspection of the ch4-ch5 imagery may allow these pixels to be identified as false alarms.

7. The Autosat volcanic ash product

In collaboration with the Satellite Systems Group in Forecasting Products, the Satellite Imagery Applications Group has developed a volcanic ash detection product on Autosat. This uses the principles described in section 2. Similar products have been developed for use in other VAACs, e.g. Washington VAAC and Darwin VAAC. This is the first satellite based volcanic ash detection product to be developed for use in the London VAAC.

The Autosat system receives, calibrates and reprojects AVHRR data to create 8-bit greyscale images. The calibration involves conversion from count to radiance and for infrared channels radiance to brightness temperature. Initially the volcanic ash detection product was created from these images by converting the greyscale back to brightness temperature (BT) for channels 4 and 5 and then subtracting channel 5 BT from channel 4 BT. The temperature range for the single channels is 198-308 K, therefore the temperatures were represented to the nearest 0.4 K. The incoming AVHRR data are in 10-bit format, a temperature discretisation of 0.1 K. Thus, the Autosat conversion to 8-bit images reduced the accuracy of the data.

It was recognised that the 10-bit representation of the AVHRR data should be retained for certain quantitative products on Autosat. The Satellite Systems Group have defined several 10-bit data products for specific purposes. The 10 bits are represented by 16 bit signed integers. The format of the data products consists of an Autosat header (twice the size of the header on the image products), followed by an array of data values. The size of a data product file is twice that of the equivalent image product. Table 3 shows the data products that are routinely produced for volcanic ash detection and development work.

Code	Description	Valid BT range
LI**D1	AVHRR channel 4 - channel 5 BTD	-100.0 K to + 100.0 K
LI**D4	AVHRR channel 4 BT	170.0 K to 350.0 K
LI**D5	AVHRR channel 5 BT	170.0 K to 350.0 K

Table 3. Autosat data products for volcanic ash detection and development work. Each product is given a filename consisting of the code and the time slot of the pass. The ** in the code is the area code (see text).

The values for all data products are in tenths of degrees Kelvin, for example, a BTD of -1.7 K will be represented by a value of -17 for data product D1. The data products in Table 3 have been defined for three areas: the North Atlantic (area code = ER), Icelandic area (area code = EL) and the Mediterranean area (area code = EQ). Within the Autosat system a product parameters file specifies the characteristics of each data product. These characteristics include valid temperature range, dimensions of the output, projection and the area covered. The data products can easily be changed by making alterations to this file.

The D1, D4 and D5 data products are routinely generated for every pass received from the operational NOAA polar orbiting satellites if the coverage is greater than 10% of the specified areas. The length of time between passes and coverage of the three areas varies throughout the day and from day-to-day. The Met Office is currently receiving and processing AVHRR data from NOAA 15 and NOAA 16. Figure 15 illustrates the frequency of generation of the volcanic ash product over a 48 hour period for the three areas. The information was collected when NOAA 12 and 14 were the operational satellites from which the Met Office was receiving data. The

combination of NOAA 15 and NOAA 16 are received at a similar frequency but are better spaced in time relative to each other.

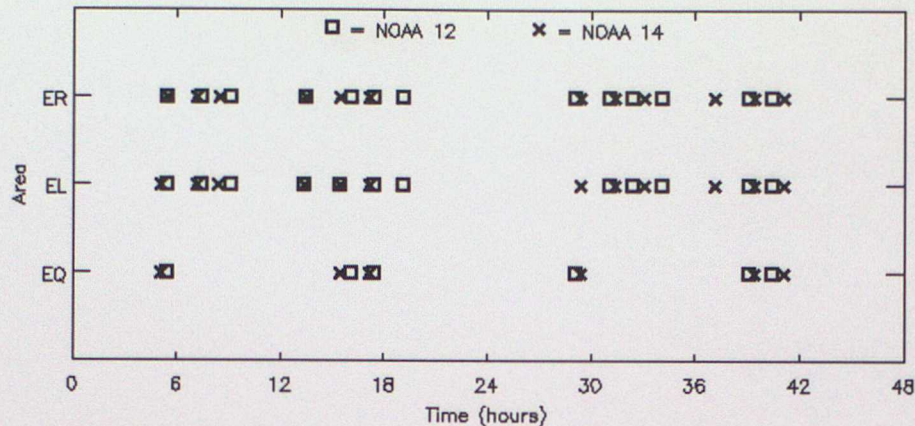


Figure 15. The plot shows the number of AVHRR ch4-ch5 images that were generated for each area over a 48 hour period starting at midnight on 17 March 2001. Area codes: ER = North Atlantic (London VAAC area); EL = Icelandic area; EQ = Mediterranean area.

Once these products are generated on Autosat they are sent to NETlink for transfer to Tigger. Tigger is a non-operational system that is used to store and display imagery on the internal web. When the channel difference product (D1) arrives on Tigger a PV-Wave program is initiated that creates GIF images from the data product. The GIF images are stored as 8-bit integer values. Due to the narrow range of expected brightness temperature differences only values between -5.0 K and +5.0 K are displayed. The discretisation of the brightness temperature differences is therefore maintained, i.e. values are displayed to the nearest 0.1 K. For display purposes brightness temperature differences below -5.0 K are set to -5.0 K, and similarly values greater than +5.0 K are set to +5.0 K. The ch4-ch5 BTG GIF images for the three areas are displayed on a Tigger volcanic ash web page. Negative ch4-ch5 BTG are represented by a colour scale from red (-0.1 K) to yellow (-5.0 K), while positive ch4-ch5 BTG are represented by a greyscale from dark grey (0.0 K) to white (+5.0 K). Pixels with ch4-ch5 BTG values lower than the threshold value of 0.0 K may contain volcanic ash. Some published studies that use ch4-ch5 BTG for volcanic ash detection use a lower threshold value (e.g. -0.5 K) so that there are a lower occurrence of false alarms. This could be considered as a development for the Autosat product for the future, but it risks eliminating some slightly negative BTG pixels that are caused by volcanic ash.

In addition to the data products, visible (channel 1) and infrared (channel 4) image products are also created for the three areas. The visible and infrared images are converted to JPEG format for areas ER and EQ and are displayed on the web page to assist with the interpretation of the ch4-ch5 BTG images. A guidance web page has been written to provide information about the data product and assistance in interpreting the imagery. This is accessible from the Tigger web pages and will allow users to gain some basic guidance on the interpretation of the imagery. Both web pages can be easily modified and updated as necessary.

The data products D4 and D5 are archived on Tigger. These products are stored on Tigger for approximately 2 months before being transferred to DAT. Code has been written to read these files and create the BTG product. The purpose of the archive is to allow unusual situations to be investigated, and to provide data for future development work.

8. Summary and suggestions for further work

A volcanic ash detection product has been developed and is automatically generated on the Autosat system at the Met Office. The product is the brightness temperature difference between channels 4 and 5 on AVHRR. It is generated for three areas, one to coincide with the London VAAC area of responsibility. From a study of volcanic clouds from 15 eruptions it was found that volcanic ash could only be detected in 6 volcanic clouds. These tended to be volcanic clouds from the large eruptions where the cloud reached a significant altitude. Several reasons why volcanic ash may not be detected have been given. Examples of volcanic clouds for which volcanic ash was and was not detected are presented. One of these was the most recent Icelandic eruption, that of Hekla in February 2000. Three situations were identified that can cause negative BTD without the presence of volcanic ash, the most frequent of these is thought to be due to the misalignment between channels 4 and 5 on AVHRR.

The current volcanic ash detection product could be improved in several ways. The use of *a priori* information about the location of volcanoes could be used in conjunction with air flow data to eliminate false alarms away from the volcano and the downwind path. Different types of volcanoes produce different types of eruptions. Examples of eruption types are: Strombolian, which typically produce little ash, and Plinian, which typically produce volcanic clouds with high ash content (Self and Walker, 1991). The classification of volcanoes in this way would enable a better understanding of what to expect when a volcano erupts and may help to explain why little or no ash was detected for a volcanic cloud. The cause of the false alarms seen in the current product could be further investigated with the aim of trying to reduce their frequency. Improvements may be possible to increase the detection rate of volcanic ash in high humidity atmospheres. Recent work by Yu, Rose and Prata (not yet published) has looked into the possibility of applying an atmospheric correction to increase the area over which volcanic ash is detected. Additional information may be gained from the 3.7 μm channel on AVHRR, either incorporated into the volcanic ash product (Ellrod and Connell, 1999), or as additional imagery to assist in the interpretation of the current product. A simple alteration to the presentation of the current ch4-ch5 imagery that may increase the ease of interpretation would be to provide an animated sequence of images.

Future developments should include the consideration of other satellite data from current and future instruments. Currently TOMS and MODIS both offer spectral information not available from AVHRR that would be of use in detecting and tracking volcanic ash clouds. The first Meteosat Second Generation satellite is due to be launched in 2002, carrying the SEVIRI (Spinning Enhanced Visible and Infrared Imager) instrument. SEVIRI possesses several channels that will be useful for detecting volcanic ash, e.g. channels at 0.6, 1.6, 3.9, 8.7, 10.8 and 12.0 μm (Watkin and Ringer, 2000), and is planned to become operational in 2002. Further work will be needed in order to exploit the capabilities of SEVIRI for volcanic ash detection. While SEVIRI will provide frequent images, being mounted on a geostationary platform, it is likely that instruments on polar orbiting satellites will continue to find application for high latitude volcanoes such as those in Iceland.

References

- Ackerman, S.A., 1997. Remote sensing aerosols using satellite infrared observations. *Journal of Geophysical Research*, **102**, no. D14, 17069-17079.
- Casadevall, T.J. and Thompson, T.B., 1995. World map of volcanoes and principal aeronautical features. *U.S. Geological Survey*.
- Constantine, E.K., Bluth, G.J.S. and Rose, W.I., 2000. TOMS and AVHRR Observations of drifting volcanic clouds from the August 1991 eruptions of Cerro Hudson. *Remote Sensing of Active Volcanism*, **116**.
- Deepak, A. and Gerber, H.E., 1983. SRA (Standard Radiation Atmosphere) Report, Section 2: Aerosol models. *Report of the experts meeting on aerosols and their climatic effects*.
- Goodrum, G., Kidwell, K.B. and Winston, W. (Editors), 2000. NOAA KLM User's guide. NOAA Climatic Data Center, Satellite Data Services Branch, Suitland, MD.
- Kidder, S.Q. and Vonder Haar, T.H., 1995. Satellite meteorology: an introduction. *Academic Press*.
- Kidwell, K.B. (Editor), 1998. NOAA Polar Orbiter data user's guide. NOAA Climatic Data Center, Satellite Data Services Branch, Suitland, MD.
- Krotkov, N.A., Toores, O., Seftor, C., Krueger, A.J., Kostinski, A., Rose, W.I., Bluth, G.J.S., Schneider, D., and Schaefer, S.J., 1999. Comparison of TOMS and AVHRR volcanic ash retrievals from the August 1992 eruption of Mt. Spurr. *Geophysical Research Letters*, **26**, no. 4, 455-458.
- Mayberry, G.C., Rose, W.I. and Bluth, G.J.S., 2000. Dynamics of the Volcanic and Meteorological Clouds Produced by the December 26, 1997 eruption of Soufriere Hills volcano, Montserrat, W.I.. *The 1995-99 eruptions of Soufriere Hills Volcano, Montserrat. Geological Society of London publication edited by Druitt, T., Young, S. and Kokelaar, P.*
- McPeters, R., Bhartia, P.K., Krueger, A., Herman, J., Wellemeyer, C., Seftor, C., Jaross, G., Torres, O., Moy, L., Labow, G., Byerly, W., Taylor, S., Swissler, T. and Cebula, R., 1998. Earth Probe Total Ozone Mapping Spectrometer (TOMS) data product users' guide. *NASA Reference Publication*, TP-1998-206895.
- Oppenheimer, C., 1998. Volcanic applications of meteorological satellites. *International Journal of Remote Sensing*, **19**, no. 15, 2829-2864.
- Prata, A.J., 1989. Observations of volcanic ash clouds in the 10-12 μ m window using AVHRR/2 data. *International Journal of Remote Sensing*, **19**, 2829-2864.
- Rose, W.I., Delene, D.J., Schneider, D.J., Bluth, G.J.S., Krueger, A.J., Sprod, I., McKee, C., Davies, H.L. and Ernst, G.J., 1995. Ice in the 1994 Rabaul eruption cloud: implications for volcanic hazard and atmospheric effects. *Nature*, **375**, 477-479.
- Rose, W.I., Bluth, G., Riley, C., Watson, M., Yu, T., and Ernst, G.G., 2000. Potential Mitigation of Volcanic Cloud Hazards using Satellite Data: a Case Study of the February 2000 Hekla Event and an Unexpected NASA DC8 encounter. *Eos Trans. AGU*, **81** (48), *Fall Meeting Supplement*.

Rose, W.I. and Mayberry, G.C., 2000. Use of GOES thermal infrared imagery for eruption scale measurements, Soufriere Hills, Montserrat. *Submitted to Geophysical Research Letters*.

Rose, W.I. and Prata, A.J., 1997, Atmospheric corrections for two band infrared volcanic cloud discriminations and retrievals. *EOS Trans AGU, Fall Meeting Abstracts*, F 818.

Schneider, D.J., Rose, W.I., Coke, L.R., Bluth, G.J.S., Sprod, I.E. and Krueger, A.J., 1999. Early evolution of a stratospheric volcanic eruption cloud as observed with TOMS and AVHRR. *Journal of Geophysical Research*, **104**, no.D4, 4037-4050.

Seftor, C.J., Hsu, N.C., Herman, J.R., Bhartia, P.K., Torres, O., Rose, W.I., Schneider, D.J. and Krotkov, N., 1997. Detection of volcanic ash clouds from Nimbus 7/total ozone mapping spectrometer. *Journal of Geophysical Research*, **102**, no. D14, 16749-16759.

Self, S. and Walker, G.P.L, 1991. Ash clouds: Characteristics of eruption columns. *Proceedings of the First International Symposium on Volcanic Ash and Aviation Safety, U.S. Geological Survey Bulletin 2047*.

Warren, S.G., 1984. Optical constants of ice from the ultra-violet to the microwave. *Applied Optics*, **23**, no.8.

Watkin, S.C. and Ringer, M.A., 2000. Investigation into the use of SEVIRI imagery for the automatic detection of volcanic ash clouds. *Met Office Forecasting Research Technical Report No. 297*.

Wen, S. and Rose, W.I., 1994. Retrieval of sizes and total masses of particles in volcanic clouds using AVHRR bands 4 and 5. *Journal of Geophysical Research*, **99**, 5421-5431.

Internet references

Alaska Volcano Observatory	www.avo.alaska.edu/
MODIS UCBS Emissivity Library	www.ices.ucsb.edu/~zhang/EMIS/html/em.html
NOAA KLM User's guide	www2.ncdc.noaa.gov/docs/podug/index.htm
NOAA Polar Orbiter data user's guide	www2.ncdc.noaa.gov/docs/podug/index.htm
NOAA's Satellite Active Archive	www.saa.noaa.gov/new-bin/WWWdisplay
TOMS SO2 and Ash Group (NASA GSFC)	skye.gsfc.nasa.gov/
Smithsonian Institute	www.volcano.si.edu/gvp/
Washington VAAC	www.ssd.noaa.gov/VAAC/washington.html

Glossary

AI	Aerosol index (from TOMS data)
AVHRR	Advanced Very High Resolution Radiometer
BT	Brightness temperature
BTD	Brightness temperature difference
EMARC	Environment Monitoring and Response Centre
FOV	Field of view
GAC	Global area coverage
GIF	Graphics Interchange Format (an image format)
JPEG	Joint Photographic Experts Group (an image format)
LAC	Local area coverage
MODIS	Moderate Resolution Imaging Spectrometer
MSG	Meteosat Second Generation
NAME	Nuclear Accident ModEl
NMC	National Meteorological Centre (at the Met Office)
NOAA	National Oceanic and Atmospheric Administration
SAA	Satellite Active Archive
SEVIRI	Spinning Enhanced Visible and Infrared Imager
SOI	Sulphur dioxide index
TOMS	Total Ozone Mapping Spectrometer
UTC	Universal time (Co-ordinated)
VAAC	Volcanic Ash Advisory Centre

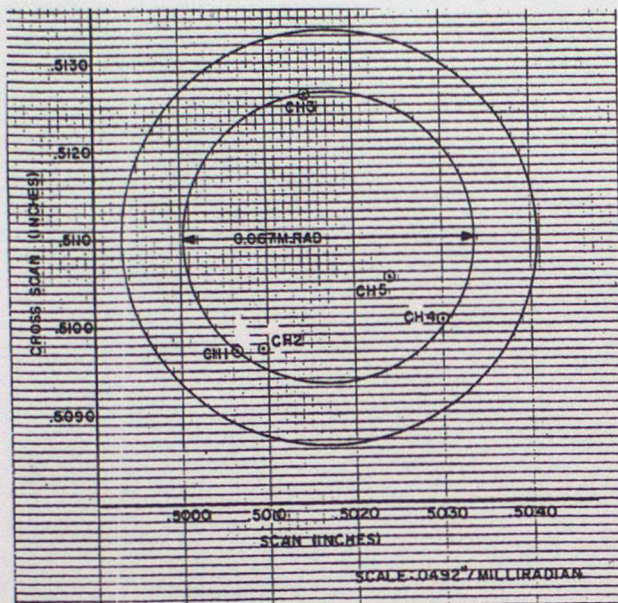
Acknowledgements

This project to develop a volcanic ash detection product was requested and supported by the Civil Aviation Branch of the Met Office Business Division.

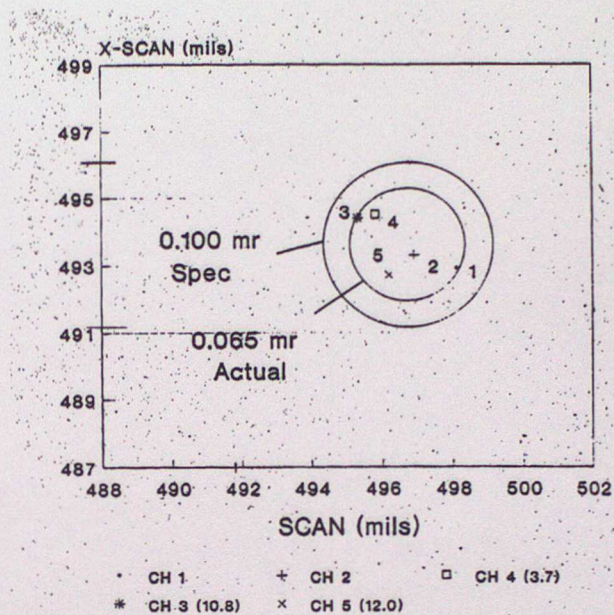
The author wishes to thank Katherine Kidwell at the National Climatic Data Center, NOAA for her helpfulness in providing the AVHRR FOV plots and information about them. Thanks are also due to Ian Brown, Ian Morgan and Freya Cromarty in Satellite Systems for their work in getting the Autosat volcanic ash product up and running, and to Bryan Conway and Roger Saunders in Satellite Applications for useful discussions and suggestions during the course of this project.

Appendix

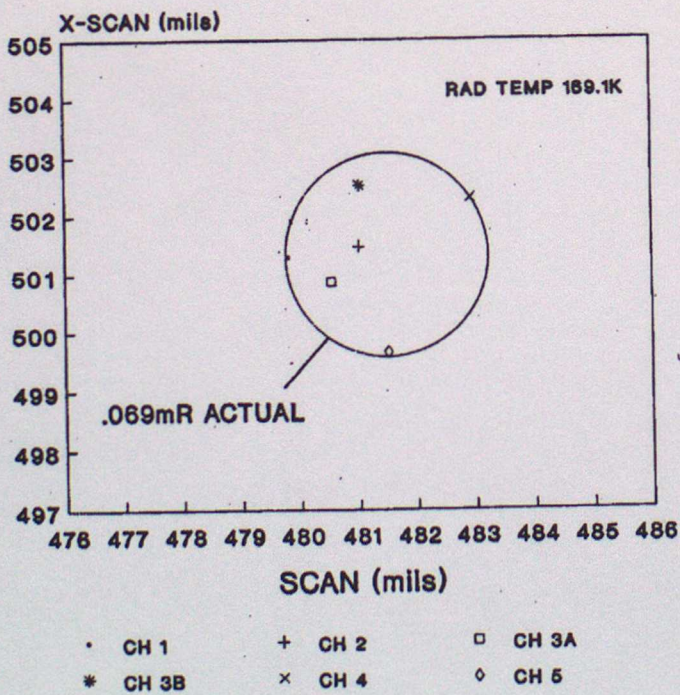
Plots of the centres of the field of views for channels on AVHRR. The measurements are for the individual AVHRR instrument on the NOAA 12, 14, 15 and 16 satellites. From National Climatic Data Center, NOAA.



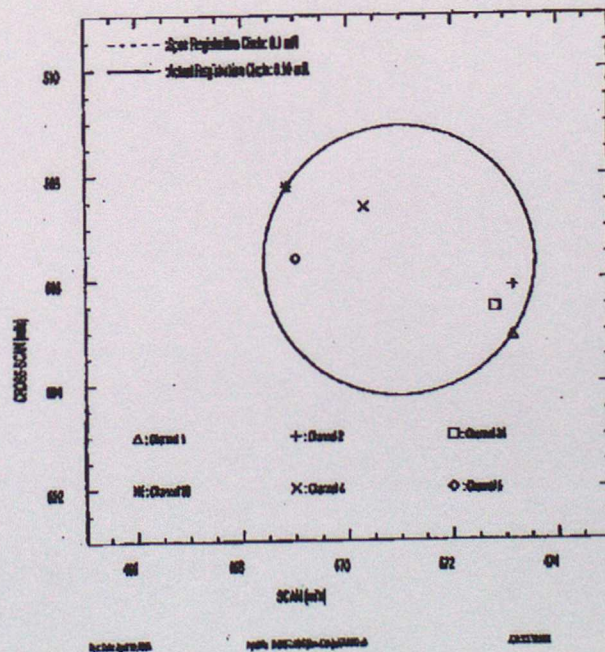
NOAA 12



NOAA 14



NOAA 15



NOAA 16